Available online at www.sciencedirect.com
SCIENCE DIRECT®
Physica C 385 (2003) 373–382
PHYSICA C
www.elsevier.com/locate/physc

Effect of Fe substitution in the structure and superconducting properties of the $(Y_{0.8}Pr_{0.2})Ba_2Cu_{4-x}Fe_xO_8$ system

R. Escamilla [a], T. Akachi [a,*], R. Gómez [b], V. Marquina [b], M.L. Marquina [b], R. Ridaura [b]

[a] *Instituto de Investigaciones en Materiales, Circuito Exterior, C.U. UNAM, Apdo. Postal 70-360, D.F. 04510 Mexico, Mexico*
[b] *Facultad de Ciencias, UNAM, D.F. 04510 Mexico, Mexico*

Received 16 April 2002; accepted 23 September 2002

Abstract

The effects of iron substitutions on the superconducting and structural properties of $(Y_{0.8}Pr_{0.2})Ba_2Cu_{4-x}Fe_xO_8$ were studied. As iron concentration increases, the rate at which T_c diminishes with x is the same as for the $YBa_2Cu_{4-x}Fe_xO_8$ system, but faster than in the $YBa_2Cu_{3-x}Fe_xO_{7-\delta}$ system. The Mössbauer spectra of the different samples, together with Rietveld refinements of their corresponding X-ray spectra, indicate that the iron atoms occupy preferably the Cu(1) sites of the double $(CuO)_2$ chains in fivefold coordination; that is, due to their tri-valency, the iron atoms attract extra oxygen atoms, named O(5), that place themselves along the a-axis in between two adjacent planes of the double $(CuO)_2$ chains. As x is increased, the Cu(1)–O(4) bond length decreases, whereas the Cu(2)–O(4) one increases. Also, a reduction of the occupation factors of the oxygen atoms in the CuO_2 planes is observed. Some of these changes may be due to the presence of O(5) atoms, which in turn affect the charge-transfer mechanism between the $(CuO)_2$ double chains and the CuO_2 planes where superconductivity takes place, and could be responsible of the rate at which T_c decreases.

PACS: 74.25; 74.10; 74.62; 76.80
Keywords: High-T_c superconductors; Y124 and (Y,Pr)124 systems; Iron substitution; T_c degradation; Mössbauer spectroscopy; Rietveld refinement; Site occupancy

1. Introduction

As a result of the many studies regarding the structural and physical properties of the $YBa_2Cu_4O_8$, Y124, it is now well known that the Y124 crystal structure is closely related to that of the $YBa_2Cu_3O_{7-\delta}$, Y123, with double $(CuO)_2$ chains, instead of single ones, along the b-axis of the unit cell [1,2]. In consequence, the c lattice parameter is longer in the former (27.25 Å) than in the later (11.68 Å). Among the isostructural compounds of the $RBa_2Cu_4O_8$ (R = rare earth) system, T_c remains essentially unchanged for all R ions regardless of

* Corresponding author. Tel.: +525-556-224633; fax: +525-556-160754.
E-mail address: tatsuo@servidor.unam.mx (T. Akachi).

0921-4534/02/$ - see front matter
PII: S0921-4534(02)02067-1

their magnetic moment, except for R = Pr [3,4]. Several studies on the $(Y_{1-y}Pr_y)Ba_2Cu_3O_{7-\delta}$ series, (Y,Pr)123, have been made [5–14]; however, there are few reports on $(Y_{1-y}Pr_y)Ba_2Cu_4O_8$, (Y,Pr)124 [15–19]. These studies show that as the Pr concentration (y) increases, T_c decreases continuously and the critical y_{cr} value at which the superconducting state disappears is larger in (Y,Pr)124 ($y_{cr} \approx 0.72$) than in (Y,Pr)123 ($y_{cr} \approx 0.55$) [20,21].

Since the discovery of high-temperature superconductivity, many experiments have been concerned with the effects that different substitutions have on their superconducting properties. It was hoped that these investigations would reveal clues on the mechanism causing the high critical temperatures in these materials. In contrast with the almost general interchangeability of the rare earths, the effects that substitutions of Cu by other 3d metals have in T_c are noticeable. However, it is still not clear what causes the degradation of T_c as dopant concentration is increased. Among the most common effects proposed in the literature are magnetic pair breaking, change in the local symmetry and purely electronic dynamical mechanisms [22]. In any case, basic issues, such as dopant site localization and charge state, must be considered.

When Fe atoms substitute a fraction of the Cu atoms, Mössbauer spectroscopy can give important information about the local electric and magnetic environment of the Cu sites where the Fe atoms are expected to reside and also about their ionic and spin states.

The main objectives of the present research are to determine where the iron atoms go into the structure of the $(Y_{0.8}Pr_{0.2})Ba_2Cu_{4-x}Fe_xO_8$ system, (Y,Pr)124Fe, how they affect its crystalline structure and transport properties, and the role played by the Pr atoms.

To achieve these objectives, substitutional studies on $(Y_{0.8}Pr_{0.2})Ba_2Cu_{4-x}Fe_xO_8$ for different x values, were carried out and our results were compared with previous results on $YBa_2Cu_{4-x}Fe_xO_8$, Y124Fe, and on $YBa_2Cu_{3-x}Fe_xO_{7-\delta}$, Y123Fe, systems. We present resistance vs. temperature measurements, X-ray diffractograms and Mössbauer spectroscopy results. Through a Rietveld refinement of the X-ray diffraction data the Cu(1)–O(4) and Cu(2)–O(4) bond lengths were calculated, where Cu(1) refers to the copper atoms in the chains, Cu(2) to those in the CuO_2 planes, and O(4) to the apical oxygen atoms that link the CuO_2 planes with the $(CuO)_2$ double chains. We also perform a calculation of the quadrupole splittings expected for different oxygen environments around the Fe atoms and, together with the occupation factors obtained from the Rietveld refinement, a site assignment of the Fe atoms is proposed.

2. Experimental

We synthesized $(Y_{0.8}Pr_{0.2})Ba_2Cu_{4-x}Fe_xO_8$ samples with $x = 0.025$, 0.05, 0.075 and 0.1 at ambient oxygen pressure [23–25] using the $(Y_{0.8}Pr_{0.2})Ba_2Cu_3O_{7-\delta}$ compound as precursor. The precursor was synthesized by the usual solid-state reaction method, using powders of Y_2O_3, $BaCO_3$, CuO and Pr_6O_{11} with 99.999% purity. Powders of $(Y_{0.8}Pr_{0.2})Ba_2Cu_3O_{7-\delta}$, CuO and $^{57}Fe_2O_3$ were mixed in stoichiometric quantities and grounded in an agate mortar. These powders were subsequently mixed with grounded sodium nitrate crystals (20% in weight) as catalyst to accelerate the reaction, pressed into pellets, heat-treated at 790 °C during 20 h in flowing oxygen and slowly cooled (0.5 °C/min) to room temperature. The heating process was repeated until the X-ray diffraction patterns showed mainly 124 phases for each iron concentration.

The crystallographic phase identification of the samples was done with a Siemens X-ray diffractometer using CuK_α radiation. The crystallographic parameters of the (Y,Pr)124Fe compounds were determined from the Rietveld refinement of the powdered X-ray diffraction data, using the Rietveld refinement program RIETQUAN v2.3 [26], with multi-phase capability, in an Ammm space group. With the obtained results, a straightforward bond length calculation for the Cu(1)–O(4) and Cu(2)–O(4) bonds was done. Resistance vs. temperature curves were determined measuring the resistance by the standard four-probe technique, in a closed-cycle helium refrigerator. The superconducting transition temperatures were

obtained from this curves at zero resistance. Room temperature Mössbauer spectra of thin powdered absorbers were recorded in transmission geometry with a constant acceleration spectrometer, using a ^{57}Co in Rh source. The spectra were fitted with a constrained-least-squares program.

3. Results

Fig. 1 shows the normalized resistance vs. temperature for the studied samples; T_c decreases continuously with x and no superconducting state can be attained at $x = 0.100$. Fig. 2 shows the T_c variation with x of (Y,Pr)124Fe compared with Y123Fe [27,28] and with Y124Fe [29] systems. The T_c value (at zero resistance) of the sample with $x = 0.075$ is an extrapolation.

The main features of the powder X-ray diffraction patterns of our samples, shown in Fig. 3, correspond to the 124 structure, with small amounts of CuO, $BaCuO_2$ and 123 impurities. Fig. 4 shows the lattice parameters of the samples as a function of the Fe content. The lattice parameters obtained from the X-ray diffraction data agree, for $x = 0$, with previous results [30] on the (Y,Pr)124. As x is increased, the a-axis lattice parameter increases slightly, the one corresponding to the b-axis is essentially unchanged and the one associated with the c-axis decreases continuously. The structure of the $(Y_{0.8}Pr_{0.2})Ba_2Cu_{4-x}Fe_xO_8$ samples remains orthorhombic up to the highest doping level studied.

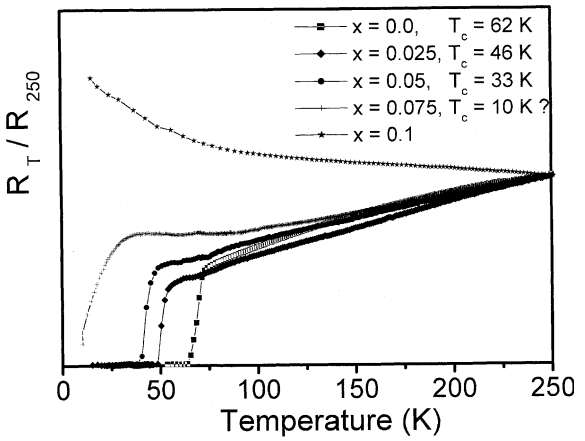

Fig. 1. Normalized resistance vs. temperature of $Y_{0.8}Pr_{0.2}Ba_2Cu_{4-x}Fe_xO_8$ samples.

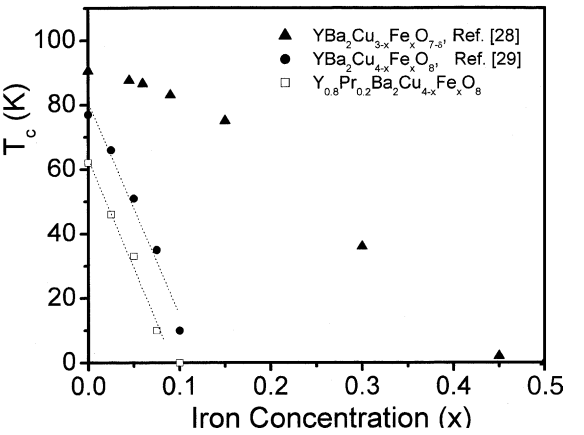

Fig. 2. T_c variation with iron concentration x of Y123Fe, Y124Fe and (Y,Pr)124Fe.

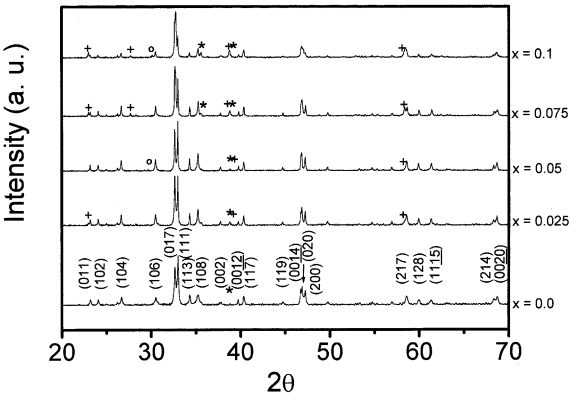

Fig. 3. X-ray diffraction patterns of the $Y_{0.8}Pr_{0.2}Ba_2Cu_{4-x}Fe_xO_8$ ($0 \leqslant x \leqslant 0.1$). The symbols (∗, +, ○) represent impurities of CuO, Y123 and $BaCuO_2$ respectively.

Powder-diffraction data were analyzed by the Rietveld technique, which allows the refinement of structural parameters and also gives information about the occupation numbers and bond lengths between different atoms in the structure. In the refinement process:

(a) It was proposed that Pr substitute for Y atoms.
(b) The presence of different impurities, such as $BaCuO_2$, CuO and 123 were considered.

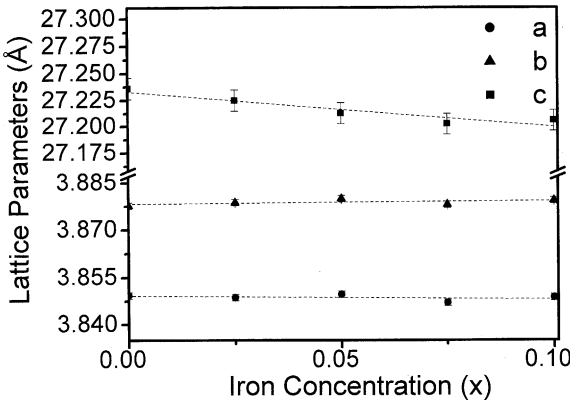

Fig. 4. Crystal lattice parameters as a function of iron concentration x.

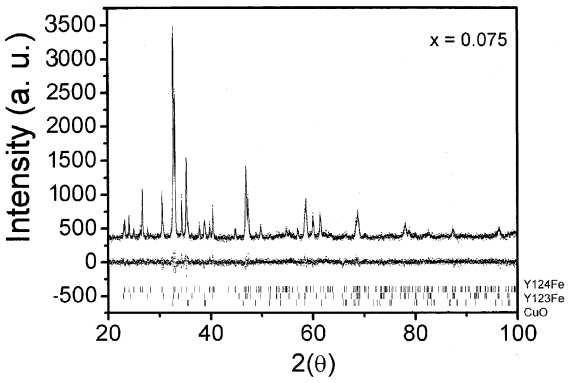

Fig. 5. Rietveld refinement on the X-ray diffraction pattern for the $x = 0.075$ sample. Experimental spectrum (dots), calculated pattern (continuous line), their difference (middle line) and the calculated peaks positions (bottom).

(c) The occupation factors of Cu and Fe atoms in the Cu(1) and Cu(2) sites were varied independently in order to allow the program to establish the site occupancy of the Fe atoms in the structure and in the impurities.

Table 1
Rietveld refinement results for the $Y_{0.8}Pr_{0.2}Ba_2Cu_{4-x}Fe_xO_8$ structure with $x = 0.075$ (panel A) and Y123 impurity (panel B)

Atom	X	Y	Z	B	N
Panel A[a]					
Cu(1)	0	0	0.2123(3)	0.5(2)	1.940(6)
Fe(1)	0	0	0.2123(3)	0.5(2)	0.052(4)
Cu(2)	0	0	0.0611(3)	1.1(2)	1.964(7)
Ba	1/2	1/2	0.1352(1)	0.15(5)	2.0
Y	1/2	1/2	0.00	1.5(2)	0.789(4)
Pr	1/2	1/2	0.00	1.5(2)	0.191(2)
O(1)	0	1/2	0.220(2)	0.5(2)	1.935(3)
O(2)	1/2	0	0.047(1)	1.1(2)	2.0
O(3)	0	1/2	0.053(1)	1.1(2)	1.908(2)
O(4)	0	1/2	0.1434(1)	0.15(5)	2.0
O(5)	0	0	0.210(3)	0.5(2)	0.052(3)
Panel B[b]					
Cu(1)	0	0	0	1.2(3)	0.963(2)
Fe(1)	0	0	0	1.2(3)	0.015(2)
Cu(2)	0	0	0.3607(2)	0.4(2)	1.980(4)
Fe(2)	0	0	0.3607(2)	0.4(2)	0.004(1)
Ba	1/2	1/2	0.1869(4)	0.5(2)	2.0
Y	1/2	1/2	1/2	0.5(2)	0.997(3)
Pr	1/2	1/2	1/2	0.5(2)	0.004(2)
O(1)	0	1/2	0	0.4(2)	0.121(2)
O(2)	1/2	0	0.3782(2)	0.4(2)	2.0
O(3)	0	1/2	0.3770(3)	0.4(2)	2.0
O(4)	0	0	0.1498(2)	0.4(2)	2.0
O(5)	1/2	0	0	0.4(2)	0.011(1)

[a] B (in Å^2) and N are the isotropic thermal and occupancy parameters. The result reliability factors were $R_{wp} = 5.6\%$, $R_E = 4.3\%$, $R_b = 5.5\%$, $S = 1.3\%$. The calculated crystal parameters (in Å) are $a = 3.8456(1)$, $b = 3.8770(1)$ and $c = 27.192(2)$.

[b] The space group is Pmmm and the calculated crystal parameters (in Å) are $a = 3.8796(3)$, $b = 3.8716(2)$ and $c = 11.597(2)$.

(d) The possibility of two extra oxygen atom positions in the structure was also consider: O(5), in between two adjacent double chains planes in front of a Cu(1) site, along the *a*-axis; and O(6), in between two adjacent CuO_2 planes above a Cu(2) site, along the *c*-axis.

As powder X-ray diffraction patterns display the same impurities for all iron concentrations, we only present the results for $x = 0.075$. Fig. 5 shows the experimental spectrum (dots), the calculated pattern (continuous line), their difference (middle pattern) and the calculated line positions (bars). In Table 1 the structural parameters obtained with the better adjustment criteria are summarized. In this table, O(1) refers to the oxygen atoms along the double chains, O(2) and O(3) to the oxygen atoms in the CuO_2 planes and O(4) to the oxygen atoms in the Ba atoms plane.

In Table 2, the (Y,Pr)124Fe occupation factors for $x = 0.075$ are summarized. This table also shows the results obtained for the 123 impurity, allowing for the presence of Pr. It is important to point out that the occupation factor of O(6) in (Y,Pr)124Fe turns out to be essentially zero for all x values. This is also the case for the occupation number of Pr in the 123 impurity. Fig. 6 shows the results of the bond length calculations for Cu(1)–O(4) and Cu(2)–O(4), and Fig. 7 shows the behavior of T_c vs. the calculated Cu(1)–O(4) bond length, both as a function of the iron concentration x.

The general aspects of the Mössbauer spectra obtained for all iron concentrations are quite similar. The ^{57}Fe Mössbauer spectra obtained were fitted with four quadrupole doublets (labeled A, B, C and D), indicating the presence of several different oxygen environments around the Fe dopant ions. Figs. 8 and 9 show the experimental data (dots), the fitted spectra (continuous line) and the

Table 2
Occupation factors for the $Y_{0.8}Pr_{0.2}Ba_2Cu_{4-x}Fe_xO_8$ sample, with $x = 0.075$ (panel A); occupation factors for the Y123 impurity of the same sample (panel B)

Panel A	
Cu(1)	1.940(6)
Fe(1)	0.052(4)
Cu(2)	1.964(7)
Fe(2)	0.00
Ba	2.00
Y	0.789(4)
Pr	0.191(2)
O(1)	1.935(3)
O(2)	2.00
O(3)	1.908(2)
O(4)	2.00
O(5)	0.052(3)
Panel B	
Cu(1)	0.963(2)
Fe(1)	0.015(2)
Cu(2)	1.980(4)
Fe(2)	0.004(1)
Ba	2.0
Y	0.997(3)
Pr	0.004(2)
O(1)	0.121
O(2)	2.00
O(3)	2.0
O(4)	2.0
O(5)	0.011(1)

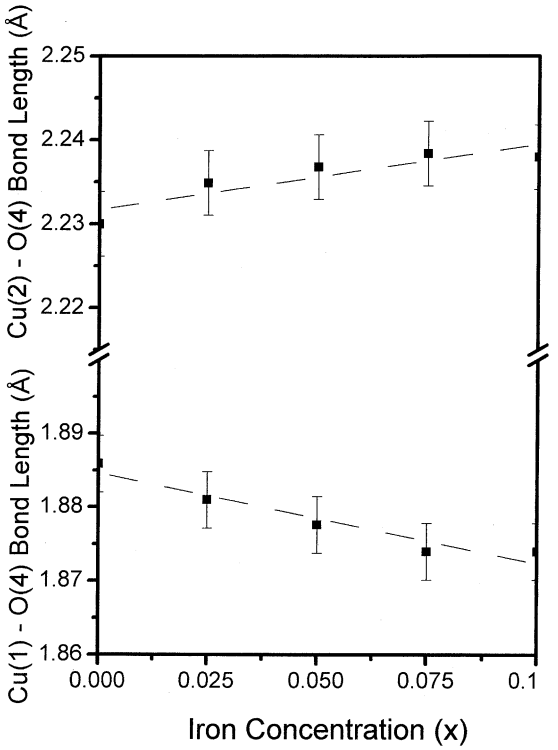

Fig. 6. Cu(1)–O(4) and Cu(2)–O(4) bond lengths vs. iron concentration x.

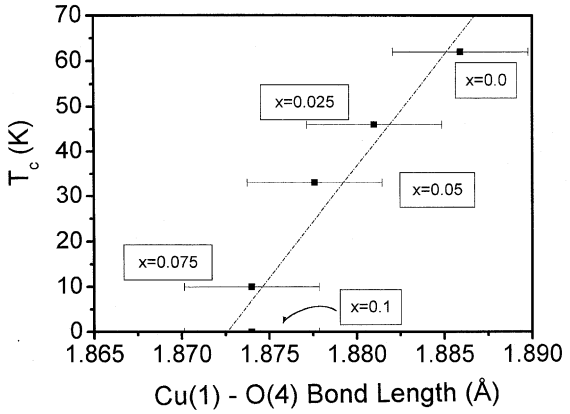

Fig. 7. T_c vs. Cu(1)–O(4) bond length for each concentration of iron.

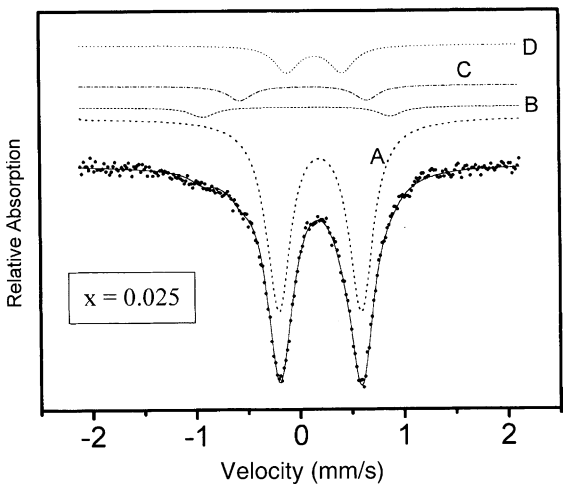

Fig. 8. Mössbauer spectra of the $x = 0.025$ sample. Experimental data (dots), fitted spectrum (continuous line) and component subspectra (broken lines).

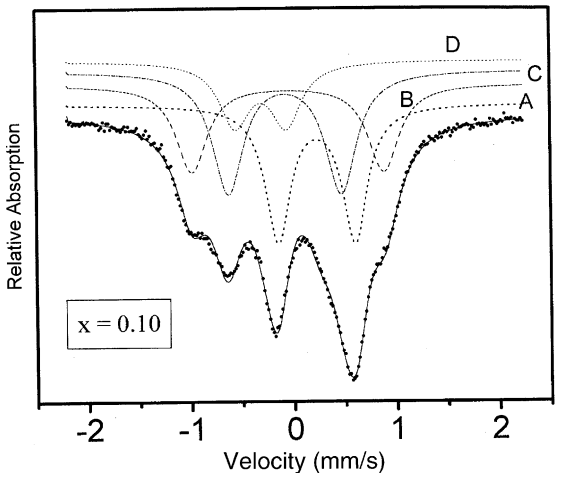

Fig. 9. Mössbauer spectra of the $x = 0.10$ sample. Experimental data (dots), fitted spectrum (continuous line) and component subspectra (broken lines).

Table 3
Mössbauer parameters of the $Y_{0.8}Pr_{0.2}Ba_2Cu_{4-x}Fe_xO_8$ system as a function of iron concentration

x	0.025	0.050	0.075	0.100
IS_A	0.31	0.30	0.31	0.32
ΔQ_A	0.79	0.83	0.77	0.76
Γ_A	0.28	0.30	0.30	0.29
IS_B	0.09	0.08	0.12	0.06
ΔQ_B	1.80	1.81	1.80	1.88
Γ_B	0.28	0.30	0.30	0.36
IS_C	0.16	0.13	0.15	0.03
ΔQ_C	1.21	1.32	1.34	1.14
Γ_C	0.28	0.30	0.30	0.36
IS_D	0.27	0.29	0.07	0.11
ΔQ_D	0.53	0.56	0.56	0.50
Γ_D	0.28	0.30	0.35	0.36

four component sub-spectra (dashed lines) for the lowest and highest iron concentrations, respectively. In Table 3, we summarize the Mössbauer parameters: quadrupole splitting (ΔQ), isomer shift (IS) and line width (Γ) for all the studied samples.

4. Discussion

Before beginning the discussion of the present results, it is worthwhile to recall that the presence of impurities and defects is common in Y124Fe, (Y,Pr)124 and (Y,Pr)124Fe samples synthesized by different methods [20,31,32]. Actually, in a high resolution transmission electron microscopy (HRTEM) study, Yanagisawa et al. [31] report that the substitution of Cu by Fe in the Y124 provokes the replacement of $(CuO)_2$ double chains by single (CuO) chains, an effect that they called "destabilization". On the other hand, Hashimoto et al. [32], also using HRTEM, account for the presence of Y123 defects in (Y,Pr)124, indicative of similar destabilization effect, produced by Pr, in

replacing double chains by single ones during the synthesis procedure.

4.1. Resistance vs. temperature

The T_c variation with x in the Y123Fe system, first shows a linear drop and then a sharp fall for $x > 0.15$ [33]. The abrupt change in the slope has been attributed to the increased Fe occupation in the Cu(2) sites of that structure. The T_c variation with x in the (Y,Pr)124Fe system is linear and has the same slope (Fig. 2) that the one observed in Y124Fe [29]. No abrupt change of slope is observed in either of these last two systems in all the x range where a T_c exists. These facts suggest that, as in Y124Fe, the Fe atoms occupy mainly one of the two possible sites of the structure. In Refs. [29,34], the double chain Cu(1) sites assignation is justified. If this is the case for $Y_{0.8}Pr_{0.2}Ba_2Cu_{4-x}Fe_xO_8$, consistent results must be obtained throughout our study.

4.2. X-ray diffraction and Rietveld refinement

An important thing to note in the X-ray diffraction patterns is the presence of a 123 impurity, even in the lowest iron concentration sample (in contrast with the Y124Fe case, where this impurity is only detected at high iron concentrations) and that the relative intensities of the peaks associated with them increase with x. The presence of this impurity is likely to be associated with a Pr–Fe combined destabilization effect of the double chains into single ones.

In the Rietveld refinements the presence of (Y,Pr)123 was taken into account. As was said before, the occupation factors obtained from this refinements for Pr in the (Y,Pr)123 structure are close to zero, indicating an almost complete reaction in the sample preparation procedure. A similar analysis in (Y,Pr)124Fe shows that the Fe atoms substitute copper atoms in the Cu(1) sites of the double chains. To less extent, iron atoms also occupy the Cu(2) sites of CuO_2 planes and the Cu(1) sites of the single chains in the Y123 impurity. The occupation factor for O(5) increases with iron concentration and the one for O(6) is essentially zero for all iron concentrations. It is important to note that the O(3) and O(1) occupation factors, when $x = 0$, are less than 2 and they diminish as x increases, as has been observed by several groups [35,36].

The Rietveld refinement made also gives information about the bond length between the atoms of the structure. A striking result is that the bond length calculations for Cu(1)–O(4) and Cu(2)–O(4) show that the former decreases whilst the latter increases with iron concentration (see Fig. 6), indicating that the O(4) atoms move towards the double chains. The above results are some how similar to the results of Awana et al. [37] for the $(Er_{1-y}Ca_y)Ba_2Cu_3O_{7-\delta}$ system as they increase the calcium concentration.

It has been claimed that the enhancement of T_c in Y124 under pressure is principally due to the substantial shortening of the Cu(2)–O(4) bond length and to the relative elongation of the Cu(1)–O(4) bond length [38,39]. These changes in bond lengths were related to the charge-carriers transfer from the $(CuO)_2$ chains to the conducting CuO_2 plane, which causes an increase in charge carriers, thus leading to an increase in T_c [40–42]. Our results show opposite variations of these same bond lengths as iron concentration is increased. According to the charge-transfer model one should expect a less effective charge transfer in the (Y,Pr)Fe system, leading to the depletion of T_c.

4.3. Mössbauer spectroscopy

With the above information and with a quadrupole splitting calculations similar to that used by Akachi et al. [29] associated with different oxygen configurations around an iron atom on the Y124Fe system, we can analyze the Mössbauer results and propose a site assignment for the Fe atoms. At this point it is important to emphasize that any quadrupole splitting calculation must be taken only as guide in the site assignment, due to the many factors that affect it. However, if one assumes that the nature of the iron bonds with their neighbor atoms has essentially the same character, the relative magnitudes of calculated quadrupole splittings must be similar to the relative magnitudes of the experimental splittings.

The Mössbauer spectra of (Y,Pr)124Fe always consists of four quadrupole doublets, in contrast with the Mössbauer spectra of Y124Fe, which shows only one quadrupole doublet up to $x \approx 0.05$ [29], implying that even at low iron concentrations, different sites of (Y,Pr)124Fe structure can be occupied by the Fe atoms.

Table 3 shows that the four quadrupole splittings observed in the Mössbauer spectra of our samples have values close to those observed in the Y124Fe system for high-iron concentrations ($x \geqslant 0.100$) [29]. The quadrupole splitting of the main doublet A (≈0.77 mm/s) is equal to that of the main doublet in the iron doped Y124 system. The quadrupole splittings of doublets B (≈1.80 mm/s) and C (≈1.34 mm/s) have values close to those associated with Fe^{3+} occupying Cu(1) sites of the single chains of the Y123 system. Finally, the quadrupole splitting of doublet D (≈0.56 mm/s) has been attributed to Fe in the Cu(2) sites of Y123Fe.

Table 4 shows the results for the quadrupole splittings calculated with a point charge model using the ionic distances obtained from the refined X-ray data. Under the assumption that the main doublet, A, is associated with Fe atoms in the Cu(1) sites of the double $(CuO)_2$ chains, the Sternheimer factor can be fixed so as to give the experimental result. The Fe atoms in these sites can be in three possible coordination states: fourfold planar, fivefold pyramidal and sixfold octahedral. The last possibility must be ruled out, because the quadrupole splitting associated with such a highly symmetrical environment is much too small. The other two give the following Sternheimer factors: 2.85 and 5.46, respectively. If one uses these values to calculate the rest of the quadrupole splittings in the Cu(1) sites, only the second one of them gives results consistent with the experimental splittings observed in the spectra.

Table 4
Quadrupole splitting calculation for different iron environments

Coordination	ΔQ (mm/s)	ΔQ (mm/s)
$YBa_2Cu_{3-x}Fe_xO_\delta$ (Fe^{3+} in Cu(1) sites)		$(1-\gamma_\infty) = 5.46$
2	$0.182(1-\gamma_\infty)$	0.99
3	$0.319(1-\gamma_\infty)$	1.74
4 (planar)	$0.325(1-\gamma_\infty)$	1.77
4 (non planar)	$0.233(1-\gamma_\infty)$	1.27
5 (pyramidal)	$0.202(1-\gamma_\infty)$	1.10
6 (octahedral)	$0.101(1-\gamma_\infty)$	0.55
Fe^{2+} in Cu(2) sites		$(1-\gamma'_\infty) = 2.63$
5 (pyramidal)	$0.198(1-\gamma'_\infty)$	0.52
($Y_{0.8}Pr_{0.2}$)$Ba_2Cu_{4-x}Fe_xO_\delta$ (Fe^{3+} in Cu(1) sites)		$(1-\gamma_\infty) = 5.46$
4 (planar)	$0.270(1-\gamma_\infty)$	1.47
5 (pyramidal)	$0.141(1-\gamma_\infty)$	0.77
6 (octahedral)	$0.030(1-\gamma_\infty)$	0.16
Fe^{2+} in Cu(2) sites		$(1-\gamma'_\infty) = 2.63$
5	$0.172(1-\gamma'_\infty)$	0.45

If doublet D is due to iron atoms in the Cu(1) sites in the Y123Fe structure, the only possibility compatible with its quadrupole splitting value is a sixfold octahedral coordination, but this is incompatible with the (essentially) zero occupation number of the O(5) sites obtained from the Rietveld refinement for the 123 structure. The other possibility is that this doublet is associated with Fe atoms in the Cu(2) sites of the structure. However, one has to use a smaller Sternheimer factor to reproduce the experimental value of the quadrupole splitting. Remembering that it is a anti-shielding factor and that the Y and Pr atoms are close to the CuO_2 planes, changes in the electronic distribution around the Fe atoms (with respect to the CuO chains) could be expected and these, in turn, would modify its value.

In consequence, the following assignment is proposed:

(a) The main doublet A (≈0.77 mm/s) is associated with Fe^{3+} atoms in the Cu(1) sites in fivefold coordination, resulting from extra oxygen atoms, named O(5), that are attracted by Fe atoms at the Cu(1) sites, and occupy sites placed along the *a*-axis between two double chains. Actually, the fact that the occupation number of O(5) is different from zero at the lowest Fe concentration is consistent with this assignment.
(b) Doublet B (≈1.80 mm/s) is associated with Fe^{3+} in the Cu(1) sites with fourfold planar coordination in the Y123 impurity [29].
(c) Doublet C (≈1.34 mm/s) is associated with Fe^{3+} also in the Cu(1) sites with fourfold (non-planar) coordination, again in the Y123 impurity.

(d) Doublet D (≈0.56 mm/s) is associated with Fe^{2+} or Fe^{3+} in the square pyramidal Cu(2) sites.

5. Conclusions

Our resistance vs. temperature measurements show that the transition temperature T_c of the $(Y_{0.8}Pr_{0.2})Ba_2Cu_{4-x}Fe_xO_8$ samples decreases linearly with increasing iron concentration x, as in the $YBa_2Cu_{4-x}Fe_xO_8$, and that the reduction rate of T_c is faster than that in $YBa_2Cu_{3-x}Fe_xO_{7-\delta}$. The Mössbauer spectroscopy results as well as the Rietveld refinement study of the crystal structure show that, for $0.025 \leqslant x \leqslant 0.10$, the iron atoms occupy mainly the Cu(1) sites of the $(Y_{0.8}Pr_{0.2})Ba_2Cu_{4-x}Fe_xO_8$ structure and, to less extent, the Cu(1) sites of the Y123 impurity and the Cu(2) sites common to both structures. The presence of the Y123 impurity (even at the lowest iron concentrations) in the (Y,Pr)124Fe system, together with the smaller than 2 occupation factors of O(3) and O(1), suggest that the presence of the Pr atoms accelerates the destabilization of double chains in the $(Y_{0.8}Pr_{0.2})Ba_2Cu_{4-x}Fe_xO_8$ system compared with the $YBa_2Cu_{4-x}Fe_xO_8$ system.

Furthermore, our results of the Rietveld refinement indicate that the Fe atoms that substitute in Cu(1) sites of the double chains attract, due to their tri-valency, extra oxygen atoms, O(5), that place themselves along the a-axis in between two adjacent planes of the double $(CuO)_2$ chains. The presence of extra oxygen atoms can affect the charge-transfer mechanism between the $(CuO)_2$ double chains and the CuO_2 planes, where superconductivity takes place, and this can manifest itself as a change in the Cu(1)–O(4) and Cu(2)–O(4) bond lengths, as well as in the rate at which T_c decreases.

In summary, the T_c degradation in the (Y,Pr)-124Fe system may have two causes:

(a) The presence of Fe and Pr atoms in the original Y124 system favours the destabilization of the $(CuO)_2$ double chains generating structural defects in the system.
(b) The substitution of Fe atoms in the Cu(1) sites modifies the charge-transfer mechanism, through excess oxygen atoms, between the double chains and the CuO_2 planes, and this may be the cause of the rapid T_c degradation with iron concentration.

Acknowledgements

The authors acknowledge I. Kaplan and M. de Llano for their help in the manuscript preparation and to M.A. Jaime and T.M. Martínez for assistance in sample preparation.

References

[1] H. Zandbergen, R. Gronsky, K. Wang, G. Thomas, Nature 331 (1988) 596.
[2] A.F. Marshall, R.W. Barton, K. Char, A. Kapitulnik, B. Oh, R.H. Harnmond, S.S. Laderman, Phys. Rev. B 37 (1988) 9353.
[3] D.E. Morris, J.H. Nickel, J.Y.T. Wei, N.G. Asmer, J.S. Scott, U.M. Scheven, C.T. Hultgen, A.G. Markelz, J.E. Post, P.J. Heany, D.R. Veblen, R.M. Hazen, Phys. Rev. B 39 (1989) 7347.
[4] K. Mori, Y. Kawaguchi, T. Ishigaki, S. Katano, S. Funahashi, Y. Hamaguchi, Physica C 219 (1994) 176.
[5] A.P. Goncalves, I.C. Santos, E.B. Lopes, R.T. Henriques, M. Almeida, M.O. Figuereido, Phys. Rev. B 37 (1988) 7476.
[6] J. Fink, N. Nucker, H. Romberg, M. Alexander, M.B. Maple, J.J. Neumeier, Phys. Rev. B 42 (1990) 4823.
[7] Y. Xu, W. Guan, Phys. Rev. B 45 (1992) 3176.
[8] H. Radousky, J. Mater. Res. 7 (1992) 1917.
[9] Y. Yamada, S. Horii, N. Yamada, Z. Guo, Y. Kodama, K. Kawamoto, U. Mizutani, I. Hirabayashi, Physica C 231 (1994) 131.
[10] N. Seiji, S. Adachi, H. Yamuachi, Physica C 231 (1994) 131.
[11] C.C. Almasan, S.H. Han, K. Yoshiara, M. Buchgeister, D.A. Gajeuski, M.L. Paulius, J. Herrmann, M.B. Maple, A.P. Paulikas, C. Gu, B.W. Veal, Phys. Rev. B 51 (1995) 3981.
[12] C.C. Almasan, M.B. Maple, Phys. Rev. B 53 (1996) 2882.
[13] C.N. Jiang, A.R. Baldwin, G.A. Levin, T. Stein, C.C. Almasan, D.A. Gajewski, S.H. Han, M.B. Maple, Phys. Rev. B 55 (1997) R3390.
[14] W.H. Tang, J. Gao, Physica C 315 (1999) 59.
[15] N. Yamada, Z. Guo, N. Ikeda, K. Kohn, T. Iri, K.I. Gondaira, Physica C 185–189 (1991) 771.
[16] T.H. Meen, Y.C. Chen, M.W. Lin, H.D. Yang, M.F. Tai, Jpn. J. Appl. Phys. 31 (1992) 3825.
[17] P. Berastegui, L.G. Johansson, M. Kall, L. Borjesson, Physica C 204 (1992) 147.
[18] Z. Guo, N. Yamada, K. Gondaira, T. Iri, K. Kohn, Physica C 220 (1994) 41.

[19] M. Kall, A.P. Litvinchuk, P. Berastegui, L.G. Johansson, L. Borjesson, M. Kakihana, M. Osada, Phys. Rev. B 53 (1996) 3590.
[20] S. Horii, Y. Yamada, H. Ikuta, N. Yamada, Y. Kodama, S. Katano, Y. Funahashi, S. Morii, A. Matsushita, T. Matsumoto, I. Hirabayashi, U. Mizutani, Physica C 302 (1998) 10.
[21] H.D. Yang, J.Y. Lin, S.S. Weng, C.W. Lin, H.L. Tsay, Y.C. Chen, T.H. Meen, T.I. Hsu, H.C. Ku, Phys. Rev. B 56 (1997) 14280.
[22] M.G. Smith, R.D. Taylor, J.D. Thompson, Physica C 208 (1993) 91.
[23] S. Adachi, T. Sugano, A. Fukuoka, N. Seiji, M. Itoh, P. Laffez, H. Yamauchi, Physica C 233 (1994) 149.
[24] C.W. Lin, J.Y. Lin, H.D. Yang, T.H. Meen, H.L. Tsay, Y.C. Chen, J.C. Huang, S.R. Sheen, M.K. Wu, Physica C 276 (1997) 225.
[25] M. Kakihana, S. Kato, V. Petrykin, J. Backstrom, L. Borjesson, M. Osada, Physica 321 (1999) 74.
[26] L. Lutterotti, P. Scardi, P. Maistrelli, J. Appl. Cryst. 25 (1992) 459.
[27] Y. Maeno, M. Kato, Y. Aoki, T. Fujita, Jpn. J. Appl. Phys. 26 (1987) L1982.
[28] C.Y. Yang, S.M. Heald, J.M. Tranquada, Y. Xu, Y.L. Wang, A.R. Moodenbaugh, D.O. Welch, M. Suenaga, Phys. Rev. B 39 (1989) 6681.
[29] T. Akachi, R. Escamilla, V. Marquina, M. Jiménez, M.L. Marquina, R. Gómez, R. Ridaura, S. Aburto, Physica C 301 (1998) 315.
[30] Y. Yamada, S. Horii, N. Yamada, Z. Guo, Y. Kodama, K. Kawamoto, U. Mizutani, I. Hirabayashi, Physica C 231 (1994) 131.
[31] K. Yanagisawa, Y. Matsui, Y. Kodama, Y. Yamada, T. Matsumoto, Physica C 183 (1991) 197, and Physica C 191 (1992) 32.
[32] K. Hashimoto, M. Akiyoshi, A. Wisniewski, M.L. Jenkins, Y. Toda, T. Yano, Physica C 269 (1996) 139.
[33] S. Katsuyama, Y. Ueda, K. Kosuge, Physica C 165 (1990) 404.
[34] I. Felner, I. Novik, B. Brosh, D. Hechel, E.R. Bauminger, Phys. Rev. B 43 (1991) 8737.
[35] A. Sequeira, H. Rajagopal, I.K. Gopalakrishnan, J.V. Yakmi, R.M. Iyer, J. Supercond. 6 (1993).
[36] K. Gopalakrishnan, J.V. Yakmi, H. Rajagopal, A. Sequeira, R.M. Yyer, Physica C 182 (1991) 67.
[37] V.P.S. Awana, S.K. Malik, W.B. Yelon, C.A. Cardoso, O.F. de Lima, A. Gupta, A. Sedky, A.V. Narlikar, Physica C 338 (2000) 197.
[38] I.D. Brown, J. Solid State Chem. 82 (1989) 122.
[39] J.D. Jorgensen, S.Y. Pei, P. Lightfoot, D.G. Hinks, B.W. Veal, B. Dabrowski, A.P. Paulikas, R. Kleb, Physica C 171 (1990) 93.
[40] E. Kaldis, P. Fischer, A.W. Hewat, E.A. Hewat, J. Karpinski, S. Rusiecki, Physica C 159 (1989) 668.
[41] R.J. Nelmes, J.S. Loveday, E. Kaldis, J. Karpinski, Physica C 172 (1992) 311.
[42] Y. Yamada, J.D. Jorgensen, S.Y. Pei, P. Lightfoot, Y. Kodama, T. Matsumoto, F. Izumi, Physica C 173 (1991) 185.